New look at AdS black holes with conformal scalar hair

Marcello Ortaggio*

Institute of Mathematics, Czech Academy of Sciences, Žitná 25, 115 67 Prague 1, Czech Republic

(Received 22 April 2024; accepted 8 July 2024; published 6 August 2024)

We revisit static, spherically symmetric solutions to anti–de Sitter (AdS)-Einstein gravity with a conformally coupled scalar field (and no self-interaction potential) in four dimensions. We first observe that a convenient choice of coordinates leads to a significant simplification of the field equations, which enables one to identify various roots of the indicial equations and thus distinct branches of solutions. Next, we construct an explicit 2-parameter hairy black hole solution in terms of an infinite power series around the event horizon. The black hole is nonextremal with a regular scalar field on and outside the event horizon, and it reduces to the Schwarzschild-AdS metric in the limit of vanishing hair. Its properties are illustrated for various values of the parameters and compared with previous numerical results by other authors. In addition, the analysis reveals the presence of a photon sphere and how the scalar field affects its size and the angular radius of the corresponding shadow. The thermodynamics of the solution is also briefly discussed.

DOI: 10.1103/PhysRevD.110.044019

I. INTRODUCTION

According to the well-known "no-hair conjecture" [1], the endpoint of gravitational collapse is expected to be a black hole completely characterized by its conserved charges—any other independent parameter ("hair") cannot be supported. While this is sustained by various no-hair theorems in electrovac General Relativity, numerous hairy black holes have been constructed in more general contexts (cf., e.g., the reviews [2,3] and [4–7] on uniqueness theorems and hairy black holes, respectively).

In particular, no-hair theorems can be bypassed if one considers a scalar field conformally coupled to gravity. Among other reasons, the interest in conformal scalar fields stems from the fact that their stress-energy has interesting properties from a quantum viewpoint [8], and it has been considered as a source in semiclassical general relativity (e.g., in [9]) and in inflationary models (cf., e.g., [10] for references). An early (static, spherically symmetric, asymptotically flat) black hole supporting a conformal scalar was discovered by Bocharova, Bronnikov, Melnikov and Bekenstein (BBMB) [11,12]. Within the same theory, an exact spherical solution in the presence of a cosmological constant $\Lambda > 0$ has been obtained more recently in [13] (dubbed MTZ in what follows), and subsequently extended to topological black holes with $\Lambda < 0$ in [14,15]. However, the solutions [13–15] require admitting also a fine-tuned quartic self-interaction (or a constant scalar field), and do not possess an independent hair parameter. It would thus be desirable to clarify if black holes with conformal hair and nonzero Λ exist also when no self-interaction is included in the theory. In such a case, according to a no-hair theorem of [16], a black hole solution conformally coupled to a scalar field with $\Lambda > 0$ cannot be asymptotically de Sitter. However, the existence of static, spherical black holes with $\Lambda < 0$ and without self-interaction has been demonstrated numerically in [16] (see also [17]).[1] But constructing a corresponding exact solution seems a challenging task, also because one needs two independent metric functions[2] to characterize such black holes [16,17] (as opposed to the solutions of [11–15]). It is the purpose of the present contribution to reconsider this problem analytically, thus providing analytic support to the numerical findings of [16,17], as well as adding several new observations (in particular regarding the presence of a photon sphere and the thermodynamics).

The plan of the paper is as follows. In the remaining part of this section we present the theory under consideration and the corresponding field equation. In Sec. II, taking advantage of conformal properties of the theory and following [22], we first cast the reduced field equations for a static, spherically symmetric ansatz in a convenient form that is considerably simpler than the one obtained in the standard Schwarzschild-like coordinates. Those will be therefore amenable to an analytic treatment, and we

*Contact author: ortaggio@math.cas.cz

[1]References [16,17] contain also results in the presence of a mass term or a self-interaction potential for the scalar field, as well as topological and higher-dimensional black holes. Some of these solutions have also been shown to be linearly stable under spherically symmetric perturbations [16,17].

[2]See Refs. [18–20] for the invariant meaning of this fact in terms of null alignment properties of the curvature, and [21] for related observations.

describe how to solve them in terms of infinite power series. This will reveal the existence of distinct branches of solutions characterized by various roots of the indicial equations and different numbers of free parameters (integration constants). By focusing on an expansion around an event horizon, in Sec. III we construct an explicit black hole solution characterized by 2 parameters (horizon radius and scalar hair), in addition to a negative Λ. Its mathematical (convergence) and physical properties (vacuum limit, asymptotic behavior, photon sphere and shadow) are discussed and further illustrated by several graphs. Some comments on the thermodynamics are also provided. Concluding remarks are given in Sec. IV. Appendix briefly discusses the energy-momentum tensor and some of the energy conditions for the hairy black hole solution of Sec. III.

We will consider the theory

$$I=\frac{1}{16\pi}\int \mathrm{d}^4x\sqrt{-g}(R-2\Lambda-S), \tag{1}$$

where S is the full trace of the following Riemann-like tensor [23]

$$S^{cd}_{ab}=\phi^2 R^{cd}_{ab}+\delta^{[c}_{[a}[-4\phi\nabla^{d]}\nabla_{b]}\phi+8(\nabla_{b]}\phi)\nabla^{d]}\phi-2\delta^{d]}_{b]}(\nabla_e\phi)\nabla^e\phi], \tag{2}$$

i.e.,[3]

$$S=S^{ab}_{ab}=\phi^2 R-6\phi\Box\phi. \tag{3}$$

Noticing that $\tilde{R}^{cd}_{ab}=\phi^{-4}S^{cd}_{ab}$ corresponds to the Riemann tensor of a conformally rescaled metric

$$\tilde{g}_{ab}=\phi^2 g_{ab}, \tag{4}$$

and $\tilde{R}^c_a=\phi^{-4}S^c_a=\phi^{-4}S^{cb}_{ab}$ to its Ricci tensor (cf., e.g., [27]), the variations of the action (1) giving rise to the tensorial and scalar field equations $E_{ab}=0$, $E_{\mathrm{s}}=0$ can be written compactly as

$$E_{ab}=G_{ab}+\Lambda g_{ab}-\phi^2\tilde{G}_{ab}, \tag{5}$$

$$E_{\mathrm{s}}=-2\phi^3\tilde{R}, \tag{6}$$

where $G_{ab}=R_{ab}-\frac{R}{2}g_{ab}$ and $\tilde{G}_{ab}=\tilde{R}_{ab}-\frac{\tilde{R}}{2}\tilde{g}_{ab}=\phi^{-2}(S_{ab}-\frac{S}{2}g_{ab})$ are the Einstein tensors of g_{ab} and $\tilde{g}_{ab}$, respectively. The term $\tilde{G}_{ab}$ in (5) is traceless after imposing $E_{\mathrm{s}}=0$ with (6), so that the trace of (5) gives $-E^a{}_a=R-4\Lambda$ (and thus $R=4\Lambda$ on shell).

II. ANSATZ AND REDUCED FIELD EQUATIONS

A. Conformally Kundt coordinates and field equations

In recent works on quadratic gravity [28,29], it has been pointed out that a convenient choice of coordinates can lead to a drastic simplification of the field equations of that theory, which proved extremely useful in the construction of black hole solutions. Since the quadratic gravity action contains a conformally invariant term, one might expect that the coordinates of [28,29] could be suitable also in other theories possessing some kind of (at least partial) conformal invariance. As observed in [22], this turns out to be the case, in particular, for the theory (1), and in the following we thus employ the conformal Kundt coordinates defined in [28,29].

We consider a metric of the form

$$\mathrm{d}s^2=\Omega^2(-2\mathrm{d}u\mathrm{d}r+H\mathrm{d}u^2+\mathrm{d}\Sigma^2),\qquad \mathrm{d}\Sigma^2=2P^{-2}\mathrm{d}\zeta\mathrm{d}\bar{\zeta},$$
$$P=1+\frac{1}{2}\zeta\bar{\zeta}, \tag{7}$$

where $\mathrm{d}\Sigma^2$ is a 2-sphere of constant Gaussian curvature normalized to 1, and we assume that Ω, H and the scalar field ϕ depend only on r. This ansatz thus includes all static metrics with spherical symmetry. The Killing vector field ∂_u is timelike where $H<0$. In the following we shall exclude from the analysis the special case $\Omega=\mathrm{const}$, which does not describe black holes since it corresponds to Kundt metrics [30]. Notice that a coordinate transformation [29,30]

$$u=\alpha^{-1}\hat{u},\qquad r=\alpha\hat{r}+\beta, \tag{8}$$

leaves the metric (7) unchanged if H is also rescaled as $H=\alpha^2\hat{H}$ ($\alpha\neq 0$ and β are constants).

We further observe that $\Omega^{-1}=0$ defines conformal infinity, provided $\nabla\Omega^{-1}\neq 0$ (and H is regular) there, and the considered spacetimes are thus asymptotically simple (at least locally) [31].[4] Note also that the Weyl invariant [29]

[3]The contribution to the integral (1) from the term $6\phi\Box\phi$ can be also written, up to a boundary term, as a standard kinetic term $-6(\nabla_a\phi)\nabla^a\phi$, as in, e.g., [8,11,24–26].

[4]Strictly speaking, this is true if, within the spacetime, one can get arbitrarily close to the hypersurface $\Omega^{-1}=0$ (without, e.g., encountering a singularity). The specific character of conformal infinity is determined by the asymptotic sign of H (i.e., Minkowskian if $H\to 0$, and (A)dS if H tends to a (negative) positive value).

$$C_{abcd}C^{abcd} = \frac{1}{3}(2+H'')^2\Omega^{-4}, \tag{9}$$

signals the presence of a possible curvature singularity at $\Omega = 0$. The spacetime is conformally flat iff $2 + H'' = 0$, and of constant curvature if, additionally, $(\Omega^{-1})'' = 0$ (hereafter a prime denotes differentiation with respect to r).

It is also interesting to point out that the coordinates (7) appear to be natural for the study of *photon spheres* [32,33], which are located at $r = r_{ps}$ such that $H'(r_{ps}) = 0$ with $H(r_{ps}) < 0$.[5] If a static observer sits at $r = r_O$ in the (static) exterior region, the angular radius χ_O of the *black hole shadow* is given by,[6]

$$\sin^2\chi_O = \frac{H(r_O)}{H(r_{ps})}. \tag{10}$$

These observations will be useful in Sec. III B.

As in [22], it proves convenient to introduce a rescaled scalar field

$$\Psi = \Omega\phi. \tag{11}$$

Using the latter, for the ansatz (7) the nonzero components of the field equations (5), (6) read

$$\frac{1}{2}\Omega^6 E^{uu} = \Omega^3(\Omega^{-1})'' - \Psi^3(\Psi^{-1})'', \tag{12}$$

$$2P^{-2}\Omega^6 E^{\zeta\bar{\zeta}} = [H(\Omega^2-\Psi^2)']' + 2\Lambda\Omega^4 - H''(\Omega^2-\Psi^2) - 6\Omega(H\Omega')' + 6\Psi(H\Psi')', \tag{13}$$

$$\Omega^6 E^{ur} = (\Omega^2-\Psi^2) - \Lambda\Omega^4 - (\Omega^{-1})'(\Omega^3 H)' + (\Psi^{-1})'(\Psi^3 H)', \tag{14}$$

$$-\frac{1}{2}\Omega^3 E_s = 6(H\Psi')' + \Psi(2+H''), \tag{15}$$

while E^{rr} is proportional to E^{ur}.

We observe that once (15) is satisfied the conservation equation [45] gives $E^{ab}{}_{,b} = 0$, which implies that (13) is not an independent equation (except in the excluded Kundt case $\Omega = \text{const}$). Keeping this into account and replacing (14) by the linear combinations $E^{ur} - \frac{1}{2}HE^{uu}$, the system of independent equations to be solved can thus be written in the simplified form

$$\Omega^3(\Omega^{-1})'' = \Psi^3(\Psi^{-1})'', \tag{16}$$

$$(\Omega^2-\Psi^2) + \frac{1}{2}[H(\Omega^2-\Psi^2)']' - \Lambda\Omega^4 = 0, \tag{17}$$

$$6(H\Psi')' + \Psi(2+H'') = 0. \tag{18}$$

This is more compact than the corresponding system in Schwarzschild coordinates [16,17,46] (defined in Sec. II B below), and as a further advantage it is an autonomous system (see Ref. [29] for similar comments in a different context).

Let us further note that two other (nonindependent) simple equations can be obtained which will be useful for practical purposes in the following. First, the trace of the Einstein equation reads

$$\Omega^4 E^a{}_a = 4\Lambda\Omega^4 - (\Omega^2-\Psi^2)(2+H'') - 6\Omega(H\Omega')' + 6\Psi(H\Psi')', \tag{19}$$

so that imposing $E^a{}_a = 0$ with (18) gives

$$6(H\Omega')' + \Omega(2+H'') - 4\Lambda\Omega^3 = 0. \tag{20}$$

Apart from the Λ term, this is a counterpart of (18), upon interchanging $\Omega \leftrightarrow \Psi$ (in the $\Lambda = 0$ case, this gives rise to the "duality" first observed in [12] and discussed recently in arbitrary dimensions in [22,47]).

In addition, using (18) and (20), the linear combination $E^{ur} - HE^{uu} = 0$ can be written as

$$[H(\Omega^2-\Psi^2)]'' - 2\Lambda\Omega^4 = 0. \tag{21}$$

The latter equation immediately reveals that for $H = 0$ one obtains $\Lambda = 0$, therefore throughout the paper we can assume $H \neq 0$, since we are interested in solutions with $\Lambda \neq 0$. For the same reason we can assume $\Omega^2 \neq \psi^2$.

B. Schwarzschild coordinates

For later discussion, let us note that metric (7) can be cast in standard Schwarzschild-like coordinates

[5]The definition of a photon spheres for static, spherically symmetric spacetimes in Schwarzschild coordinates (22), (24) reads $2f = \rho f_{,\rho}$ with $g > 0$, where both conditions must hold at the photon surface radius $\rho = \rho_{ps}$, see Ref. [34] (cf. also [32,33,35,36]). To our knowledge, the use of the conformal Kundt coordinates (7) in this context had not been considered in the literature so far—however, a "potential" which equals (up to a sign) our metric function H was conveniently defined in [35].

[6]This follows readily from Eq. (43,[37]) keeping into account the comments in footnote 5 but an equivalent formula was given earlier in [38] (cf. also [39]). For simplicity, here we have assumed there is a single photon sphere in the exterior region (as will be indeed the case in the rest of the paper, cf. Sec. III). A more general discussion, including the angular radius of shadows defined for comoving observers in asymptotically de Sitter spacetimes, can be found in [40]—cf. also the review [41] and references therein. In the special case of the Schwarzschild black hole, formula (10) was first obtained in [42,43], and extended to include Λ in [44] (see again [41] for more references and for an overview of the various terminology used in this context in the literature).

TABLE I. Summary of possible values of the exponents (n, p, q) for solutions with $\Lambda \neq 0 \neq \phi$, ordered by increasing value of n. The last column indicates the number of essential [i.e., after using the gauge freedom (8)] integration constants which characterize a given branch of solutions. It should be emphasized that, for a particular (infinite) set of $n \in \mathbb{N}^+$, there exists also a special branch with $n = q > 0$, $p < 2$ and $a_0^2 - b_0^2 = 0$ which has been omitted from this table. Such solutions do not represent expansions near a black hole horizon and will be discussed elsewhere.

(n, p, q)	Expansion at	Behavior of ϕ	Parameters
$(-1, 0, 0)$	Conformal infinity ($\rho \to \infty$)	$\phi \sim \rho^{-1}$	3
$(-1, 0, 1)$	Conformal infinity ($\rho \to \infty$)	$\phi \sim \rho^{-2}$	2
$(0, 0, 0)$	Generic point	$\phi \to$ const	4
$(0, 0, 1)$	Zero of ϕ	$\phi \to 0$	3
$(0, 1, 0)$	Nonextremal horizon	$\phi \to$ const	2
$(1, 0, 0)$	Non-Schwarzschildian Singularity	$\phi \to \infty$	3

$$\mathrm{d}s^2 = -f(\rho)\mathrm{d}t^2 + \frac{d\rho^2}{g(\rho)} + \rho^2 \mathrm{d}\Sigma^2, \tag{22}$$

via the transformation [28]

$$\mathrm{d}t = -\mathrm{d}u + \frac{\mathrm{d}r}{H}, \qquad \rho = \Omega, \tag{23}$$

giving

$$f = -\Omega^2 H, \qquad g = -\left(\frac{\Omega'}{\Omega}\right)^2 H. \tag{24}$$

In regions where $H < 0$, ∂_t is timelike and throughout the paper it will be assumed to be future oriented (so that $\partial_u = -\partial_t$ is past oriented).

We observe that the above coordinate transformation is not defined if $\Omega = \text{const}$ (corresponding to Kundt metrics) or $H = 0$—those cases are, however, not relevant to the present paper, as mentioned above.

C. Power series expansions and summary of solutions

Similarly as in [29], in order to construct analytic solutions, we will employ a Frobenius-like method (cf., e.g., [48]), which consists in expanding the unknown functions around an arbitrary, finite value of the radial coordinate $r = r_0$ as infinite power series

$$\Omega = \Delta^n \sum_{k=0} a_k \Delta^k, \quad \Psi = \Delta^q \sum_{k=0} b_k \Delta^k, \quad H = \Delta^p \sum_{k=0} c_k \Delta^k, \tag{25}$$

where $\Delta \equiv r - r_0$, and (n, p, q) and a_k, b_k and c_k are constants, with $a_0, b_0, c_0 \neq 0$. Then, by plugging (25) into the field equations (16)–(18), one is first typically able to constraint the permitted values of the exponents (n, p, q) by considering the terms of lowest orders in Δ in the resulting equations. The next step consists in using higher orders to construct a set of recurrence formulas such that the coefficients a_k, b_k and c_k in (18) for an arbitrary k are determined in terms of those with lower indices. This enables one to identify the coefficients which remain arbitrary as integration constants (the details depending on the specific solution under consideration), and to evaluate the metric functions as accurately as desired at any point within the convergence radius of the series.

Different values of (n, p, q) (i.e., the "indices" [48]) correspond to different branches of solutions. The derivation of all possible cases is straightforward but lengthy and we shall present a thorough analysis elsewhere. For the purposes of the present contribution, it suffices to only summarize here the resulting possibilities in Table I. Among those, it is easy to identify the branch $(n = 0, p = 1, q = 0)$ as an expansion around a nonextremal Killing horizon—these are thus solutions which may describe black holes and will be analyzed in the rest of the paper. We also observe that an expansion around a degenerate horizon would require $n = 0$ and $p = 2$—no such solutions are thus present in the class constructed with the above method.[7] The remaining cases will be analyzed elsewhere.

Let us further notice that the scaling freedom (8) rescales the coefficients in (25) as $\hat{a}_k = \alpha^{n+k} a_k$, $\hat{b}_k = \alpha^{q+k} b_k$ and $\hat{c}_k = \alpha^{p-2+k} c_k$, and thus always allows one to normalize arbitrarily one of those (provided it is nonvanishing), along with $\hat{r}_0 = \alpha^{-1}(r_0 - \beta)$. This will be useful in the following to get rid of one unphysical parameter and write the solutions in a canonical form.

III. BLACK HOLE SOLUTIONS: CASE $(n = 0, p = 1, q = 0)$

The focus of this paper is on black holes with a nonextremal horizon. From now on we thus study the

[7] This is due to the assumption $\Lambda \neq 0$—in the case $\Lambda = 0$ one would recover the well-known extremal solution of [11,12].

branch of solutions with exponents $(n=0, p=1, q=0)$, which means we are expanding the metric near a nonextremal Killing horizon, located at $r=r_0$. The particular value r_0 can be shifted at will by choosing β in (8) arbitrarily and has therefore no physical meaning. The physical (dimensionful) horizon radius is given in Schwarzschild coordinates (22) by the integration constant a_0 (cf. more comments in the following)

$$\rho(r_0) = a_0 > 0. \tag{26}$$

The sign of a_0 has been fixed (without losing generality) thanks to the invariance of (7) under $\Omega \to -\Omega$.

By taking an appropriate sign of α in (8) one can further also set $a_1 > 0$, such that near and across the horizon ρ is monotonically increasing with r.[8] Since our aim is to study the spacetime in the vicinity of an outer black hole horizon, we then need to assume $c_0 < 0$ (which ensures that ∂_u is timelike, cf. [49] for related comments). Hereafter we therefore restrict ourselves to the parameter range

$$a_1 > 0, \qquad c_0 < 0. \tag{27}$$

Let us emphasize that the solution obtained in the following admits any sign of Λ (see Sec. III A 1 for $\Lambda = 0$). However, because of the result of [16] mentioned in Sec. I, in the discussion of black holes we will restrict ourselves to the case $\Lambda < 0$.

A. General solution with $\Lambda \neq 0$: hairy AdS black hole

Substituting (25) with $(n=0, p=1, q=0)$ into (16)–(18) reveals that a solution in this branch is possible only for $a_0^2 - b_0^2 \neq 0$, which will thus be assumed hereafter. According to the value b_0 of the scalar field Ψ at the horizon, one can thus identify two disconnected branches of solutions, i.e., those with $a_0^2 - b_0^2 > 0$ or with $a_0^2 - b_0^2 < 0$. In the following we will be focusing mostly on the former, since it is the only one continuously connected (for $b_0 \to 0$) to the vacuum AdS black holes (and the only one giving rise a positive entropy, as discussed later on in Sec. III B 2).

At the lowest orders (16)–(18) further give

$$\begin{aligned} a_1 &= -\frac{a_0}{c_0} + \frac{a_0^3\Lambda(3a_0^2 - 2b_0^2)}{3c_0(a_0^2 - b_0^2)}, \\ a_2 &= \frac{a_0}{c_0^2} - \frac{2a_0^3\Lambda(3a_0^2 - 2b_0^2)}{3c_0^2(a_0^2 - b_0^2)} + \frac{a_0^5\Lambda^2(3a_0^2 - b_0^2)}{3c_0^2(a_0^2 - b_0^2)}, \end{aligned} \tag{28}$$

$$\begin{aligned} c_1 &= 2 - \frac{a_0^4\Lambda}{a_0^2 - b_0^2}, \\ c_2 &= \frac{1}{c_0} - \frac{4a_0^4\Lambda}{3c_0(a_0^2 - b_0^2)} + \frac{a_0^6\Lambda^2(3a_0^2 + 4b_0^2)}{9c_0(a_0^2 - b_0^2)^2}, \end{aligned} \tag{29}$$

$$\begin{aligned} b_1 &= -\frac{b_0}{c_0} + \frac{a_0^4 b_0\Lambda}{3c_0(a_0^2 - b_0^2)}, \\ b_2 &= \frac{b_0}{c_0^2} + \frac{a_0^4 b_0\Lambda(a_0^2\Lambda - 6)}{9c_0^2(a_0^2 - b_0^2)}. \end{aligned} \tag{30}$$

All higher order coefficients are then obtained recursively as

$$\begin{aligned} &k(k-1)(a_0 a_k - b_0 b_k) \\ &\quad = \sum_{j=1}^{k-1} j(2k - 3j + 1)(a_j a_{k-j} - b_j b_{k-j}), \end{aligned} \tag{31}$$

$$\begin{aligned} &k(k+1) b_0 c_k \\ &\quad = -6k^2 c_0 b_k - 2b_{k-1} - \sum_{j=1}^{k-1} c_j [6k(k-j) + j(j+1)] b_{k-j}, \end{aligned} \tag{32}$$

$$\begin{aligned} &6k^2 c_0 (a_0^2 - b_0^2) b_k \\ &\quad = 2a_0(b_0 a_{k-1} - a_0 b_{k-1}) - 4a_0 b_0 \Lambda \sum_{j=0}^{k-1} \sum_{l=0}^{k-j-1} a_j a_l a_{k-j-l-1} \\ &\qquad + \sum_{j=1}^{k-1} \left[\frac{6k}{k-1} j(2k - 3j + 1)(a_j a_{k-j} - b_j b_{k-j}) b_0 c_0 \right. \\ &\qquad \left. + [6k(k-j) + j(j+1)] a_0 c_j (b_0 a_{k-j} - a_0 b_{k-j}) \right], \end{aligned} \tag{33}$$

which thus fully determine [via (25)] the solution.

The three coefficients a_0, b_0 and c_0 remain arbitrary, but the modulus of c_0 can be rescaled as desired using (8) with $\alpha > 0$ [recall (27)]. There eventually remains two independent free physical parameters related to mass and scalar hair. Because of (27), they must obey

$$1 - \Lambda a_0^2 - \frac{\Lambda}{3} \frac{a_0^2 b_0^2}{a_0^2 - b_0^2} > 0. \tag{34}$$

For definiteness, it may also be useful to give the leading terms of the above solution in the Schwarzschild coordinates (22). This gives rise to an expansion at the horizon radius $\rho = a_0$, which is given, up to the subleading order, by

[8] Except in the special case $a_1 = 0$, which we will not consider in the following.

$$f=\frac{3a_0c_0^2(a_0^2-b_0^2)}{3(a_0^2-b_0^2)-a_0^2\Lambda(3a_0^2-2b_0^2)}(\rho-a_0)-3c_0^2(a_0^2-b_0^2)\frac{a_0^4b_0^2\Lambda^2(6a_0^2-5b_0^2)+9(a_0^2-b_0^2)[(a_0^2-b_0^2)-a_0^4\Lambda]}{[3(a_0^2-b_0^2)-a_0^2\Lambda(3a_0^2-2b_0^2)]^3}(\rho-a_0)^2+\ldots,$$
$$g=\left[\frac{1}{a_0}-\frac{\Lambda}{3}\frac{a_0(3a_0^2-2b_0^2)}{a_0^2-b_0^2}\right](\rho-a_0)-\frac{a_0^4b_0^2\Lambda^2(6a_0^2-b_0^2)+9(a_0^2-b_0^2)[(a_0^2-b_0^2)-a_0^4\Lambda]}{3a_0^2(a_0^2-b_0^2)[3(a_0^2-b_0^2)-a_0^2\Lambda(3a_0^2-2b_0^2)]}(\rho-a_0)^2+\ldots,$$
$$\phi=\frac{b_0}{a_0}+\frac{2b_0\Lambda(a_0^2-b_0^2)}{3(a_0^2-b_0^2)-a_0^2\Lambda(3a_0^2-2b_0^2)}(\rho-a_0)+\ldots, \tag{35}$$

where (34) ensures that the above denominators are nonzero. At the leading order, f and g coincide if one chooses the gauge $a_1=a_0^2$ [recall (28)]. In the special case $1-\frac{\Lambda}{3}a_0^2(3a_0^2-2b_0^2)(a_0^2-b_0^2)^{-1}=0$ (i.e., $a_1=0$), expansions in Schwarzschild coordinates need to be treated differently due to the appearance of nonintegers powers.

As mentioned in Sec. I, a result of [16] implies that, for $\Lambda>0$, the above black holes are not asymptotically de Sitter. However, numerics in the case $\Lambda<0$ shows that they are compatible with anti-de Sitter asymptotics [16,17]. Before further elucidating their properties, in the following two subsections we briefly comment on the solutions of (5), (6) [of the form (7), (25)] possessing an horizon (also) in the limits $\Lambda=0$ and $\phi=0$.

1. Limit $\Lambda=0$: Schwarzschild (stealth) solution

By setting $\Lambda=0$, one can easily prove by induction that the coefficients a_k, b_k and c_k obtained in Sec. III A satisfy

$$a_k=a_0\left(-\frac{1}{c_0}\right)^k,\qquad b_k=b_0\left(-\frac{1}{c_0}\right)^k\qquad(k\geq 0),$$
$$c_1=2,\qquad c_2=\frac{1}{c_0},\qquad c_l=0\qquad(l\geq 3). \tag{36}$$

This gives rise to series that can be summed up exactly to obtain the Schwarzschild solution with $2M=a_0$ and a constant scalar field $\phi=b_0/a_0$ (after using (8) to set $r_0=-1/a_0$, $c_0=-1/a_0$, see also Sec. VIII.B.1 of [50] for a related discussion). This is a stealth solution since $T_{ab}=0$. The outer horizon condition (34) is automatically satisfied.

This is in agreement with the known result [51–54] that there exist no nonextremal (nonstealth) black holes in the case $\Lambda=0$.

2. Limit $\phi=0$: Vacuum Schwarzschild-(A)dS black hole

In the derivation of Sec. III A we assumed $\psi\neq 0$. For a comparison, let us observe that the vacuum (A)dS black hole can in a similar way be obtained as a series expansion by solving the Eqs. (16)–(18) with $\psi=0$ (as discussed in [55]). This gives $a_k=a_0(a_1/a_0)^k$ with $a_1=a_0(\Lambda a_0^2-1)/c_0$, and $c_1=2-\Lambda a_0^2$, $c_2=(\Lambda a_0^2-3)(\Lambda a_0^2-1)/(3c_0)$, while $c_k=0$ for $k\geq 3$.[9] The parameters r_0, a_0 and c_0 remain arbitrary, but one can use (8) to set $r_0=-a_0^{-1}$ and $c_0=(\Lambda a_0^2-1)/a_0$ (i.e., $a_1=a_0^2$), thereby obtaining the standard normalization $\Omega=-1/r$, $H=-r^2+\Lambda/3+\frac{a_0}{3}(\Lambda a_0^2-3)r^3$, where the usual mass parameter is thus given by $2M=a_0(1-\frac{\Lambda}{3}a_0^2)$. For $M>0$, a photon sphere is located at $r^{-1}=-3M$, i.e., at $\rho=3M$ [32,44] in the coordinates (22).

Here (34) gives

$$1-\Lambda a_0^2>0. \tag{37}$$

Saturating the inequality in (37) (i.e., taking the limit $1-\Lambda a_0^2\to 0$) gives rise to the standard extremality condition for dS black holes [56]. When $1-\Lambda a_0^2<0$, condition (34) is violated, and the horizon $r=r_0$ cannot be an outer black hole horizon [56] (e.g., it is a cosmological one for pure dS spacetime, i.e., when $a_0^2=3/\Lambda>0$). For the Schwarzschild-AdS black hole the temperature is given by $T=\frac{1}{4\pi a_0}(1-\Lambda a_0^2)$ and the entropy by $\mathcal{S}=\pi a_0^2$ [57].

B. Properties of the solution

1. Geometry and photon sphere

The convergence properties of the series (25) with (28)–(33) can be analyzed by standard methods. In Figs. 1 and 2 we give evidence that the roots $|a_k|^{\frac{1}{k}}$ and $|c_k|^{\frac{1}{k}}$ tend to constant values for a large k (the same is true for $|b_k|^{\frac{1}{k}}$, not displayed) for specific values of the three arbitrary parameters a_0, b_0 and c_0 and of Λ. Using the root test (cf., e.g., [58]) one can thus estimate the radius of convergence of each of the series (25). We have found a qualitatively similar behavior also for some other values of the parameters.

The behavior of the metric functions Ω and H in the exterior region $\Delta>0$ and up to the convergence radius is depicted in Figs. 3 and 4. The former indicates that (at least for certain choices of the integration constants) the

[9]Here we assume $\Lambda a_0^2-1\neq 0$ to avoid solutions of the Kundt class (for which $\Omega=$ const). The special case $\Lambda a_0^2-1=0$ gives rise to the (anti-)Nariai spacetime (cf. [49]).

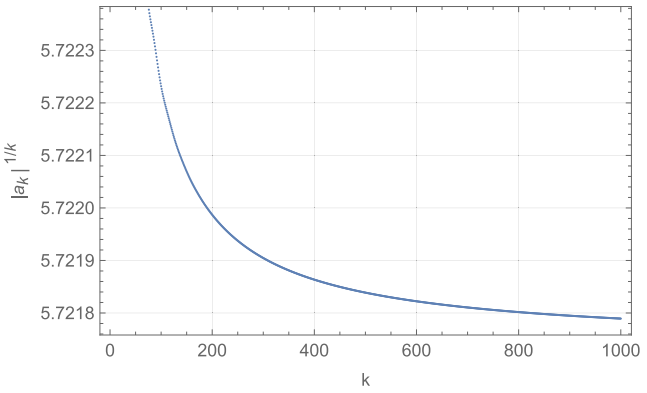

FIG. 1. Plot of $|a_k|^{\frac{1}{k}}$ against k for $k = 1, \ldots, 1000$ [cf. (31)] with parameters given by $\Lambda = -1/7$, $a_0 = 1$, $b_0 = 1/3$, $c_0 = -1/5$ (such that $a_0^2 - b_0^2 > 0$ and (27) is satisfied). From the approximate asymptotic value of $|a_k|^{\frac{1}{k}}$ one can estimate the convergence radius of the power series for Ω (Eq. (25) with $n = 0$) using the standard root test, which thus constraints the range of Δ (for the given choice of parameters) as $|\Delta| \lesssim 0.1748$.

convergence of the series breaks down near conformal infinity, where Ω blows up. The latter shows that H is regular and enables one to identify a photon sphere [32,33] at the local minimum (see Sec. II A). Furthermore, having determined the r-dependence of H, one can compute the angular radius of the black hole shadow (10) for a static observer at any $r = r_O > a_0$ (within the convergence radius).

Form a physical viewpoint, however, it is more interesting to characterize the dependence of H as a function of the

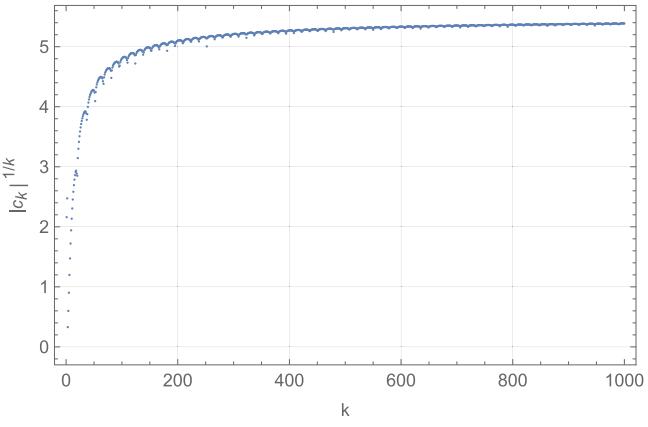

FIG. 2. The same as in Fig. 1 (with the same choice of parameters) but now for the root $|c_k|^{\frac{1}{k}}$ [cf. (32)]. In this case, the root test indicates a slightly larger convergence radius for the power series for H [Eq. (25) with $p = 1$], namely $|\Delta| \lesssim 0.1856$. A similar estimate for the convergence radius of the power series for ψ (Eq. (25) with $q = 0$) can be obtained using the ratio $|b_k|^{\frac{1}{k}}$ [cf. (33)]—we omit the corresponding plot since it would not add relevant new information. For simplicity, in the rest of the paper we will always refer to the "safer" convergence radius $|\Delta| \lesssim 0.1748$ obtained in Fig. 1.

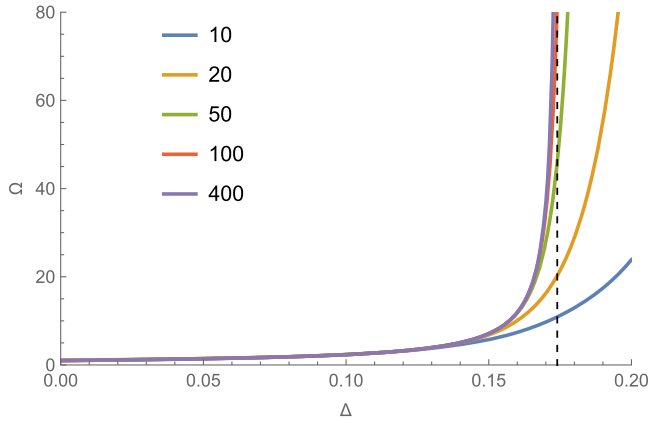

FIG. 3. Plot of Ω (Eq. (25) with $n = 0$) against $\Delta \equiv r - r_0$ in the exterior region $\Delta > 0$ with parameters as in Fig. 1. The plots are based on expansions taking into account the first 10, 20, 50, 100, and 400 terms, as indicated by the different colors. The event horizon is located at $\Delta = 0$. The dashed vertical line represents the radius of convergence as estimated in Fig. 1. The fact that Ω grows very rapidly as one approaches the radius of convergence (and as more terms of the series are kept into account) suggests that the radius of convergence (in the exterior region) is close to conformal infinity. For example, keeping into account the first 100 terms in (25) one obtains $\Omega \approx 102$ near the convergence radius (and bigger values if more terms are summed in the series).

Schwarzschild radial coordinate ρ [cf. (22), (23)] in the exterior region $\rho > a_0$, which is done in Fig. 5. First, this enables one to identify the physical radius ρ_{ps} of a photon sphere. While for vacuum black holes the ratio between ρ_{ps} and the mass M is exactly 3 (and thus independent of Λ, cf. [32,44] and Sec. III A 2, and [59] for the case $\Lambda = 0$), our findings indicate that the effect of the scalar hair is to make ρ_{ps}/M smaller, at least in the considered region of the parameter space (cf. table II, where the choice $a_0 = 1$ means a unit horizon radius; the definition of M is discussed below in the rest of this section). It can be

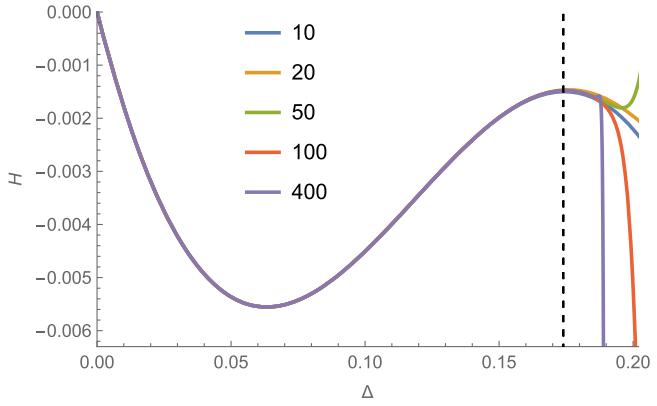

FIG. 4. The same as in Fig. 3 but here for the plot of H (eq. (25) with $p = 1$) in the exterior region. The local minimum of H located at $\Delta \simeq 0.063$ identifies a photon sphere [32,33] (cf. Sec. II A).

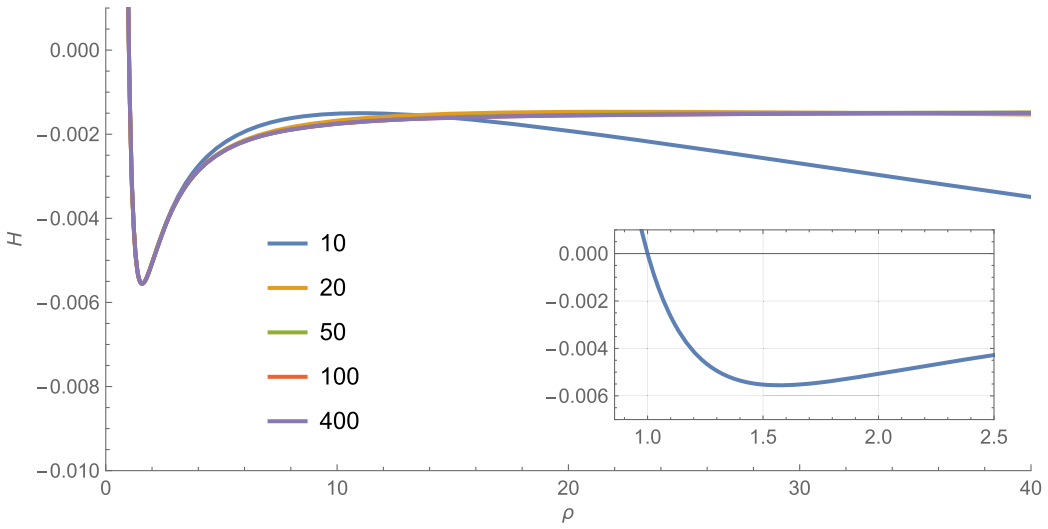

FIG. 5. The same as in Fig. 4 but H is now plotted against the Schwarzschild radial coordinate ρ, cf. (22), (23). The event horizon is located at $\rho = 1$, where $H = 0$, and the photon sphere (cf. the inset) at $\rho \simeq 1.571$. The "anomalous," decreasing part of the curve based on an expansion with only the first 10 terms corresponds to a region well beyond convergence radius, cf. Fig. 3, and should thus not be taken into account. On the other hand, expansions with a larger number of terms indicate that H tends asymptotically to a constant—i.e., the metric function f [Eq. (24)] behaves as $f \sim \rho^2$ for a large ρ, as expected in an asymptotically AdS spacetime. By considering a series with up to 1000 terms (not displayed here) we have obtained a rough estimate of the asymptotic value of $H \approx -0.00148$ (this is, however, an extrapolation based on the value of H at a distance from the horizon of about 10^3 horizon radii—a more accurate estimate may require a higher number of terms in the series, as well as a more precise knowledge of the radius of convergence).

TABLE II. The table shows the values attained by the physical quantities which characterize the AdS black hole solution (28)–(32) for different choices of Λ and of the hair parameter b_0. In particular, the shadow angular radius [cf. (10)] for a static observer close to infinity is given by χ_O^∞. In all cases we have chosen $a_0 = 1$ and fixed the gauge as $c_0 = -1/5$ (as in previous graphs) and we have approximated the solution by considering series (25) with 1000 terms. The particular choice $\Lambda = -3$, $b_0 = 0.857$ corresponds to the case considered in Fig. 2 of [17] (up to a different normalization of the scalar field and a different gauge choice in [17], which does not affect the displayed physical quantities). For comparison, vacuum Schwarzschild-AdS black holes, for which $b_0 = 0$, are also included (the corresponding exact expressions, given in Sec. III A 2, have been rounded up here to a limited number of decimal digits, which explains why the displayed ratio ρ_{ps}/M does not equals the exact value 3 [32,44]). The symbol $\simeq$ means that the displayed values of ρ_{ps} are approximate (only) because a finite number of terms are considered in the series (25), whereas $\approx$ is used for quantities that, in addition, involve an extrapolation to large values of ρ (cf. the main text and Figs. 5 and 7 for further comments). The values obtained for the latter should thus be taken with some caution and will need to be confirmed by different methods. By contrast, the displayed values of the entropy $\mathcal{S}$ (which does not depend on Λ) are based on the exact formula (39) and thus do not involve any approximation (other than rounding it up to a limited number of decimal digits). In the last row of both cases $\Lambda = -2$ and $\Lambda = -3$, the symbols ✗ denotes quantities which we have been unable to compute using the series expansion method. The reason is that, for those particular values of the parameters, the convergence radius is reached well before ρ can approach infinity—the behavior of H and its derivatives (undisplayed) near the convergence radius further suggests that the corresponding spacetimes are not asymptotically simple [31]. This is presumably due to b_0 being too close to the critical value $b_0 = 1$, and seems compatible with the rapid growth of the mass observed in [17] when $b_0 \to 1$.

Λ	b_0	$\rho_{ps}\simeq$	$M\approx$	$\rho_{ps}/M\approx$	$\sin^2\chi_O^\infty\approx$	$T\approx$	$S\approx$
	0	1.571	05.2	3.02	0.261	0.091	π
	1/3	1.571	0.77	2.04	0.267	0.090	2.79
$-\frac{1}{7}$	0.600	1.570	1.33	1.18	0.282	0.089	2.01
	0.857	1.566	2.16	0.73	0.324	0.087	0.83
	0.970	1.578	2.69	0.59	0.388	0.099	0.19
	0	2.500	0.83	3.01	0.926	0.239	π
	1/3	2.468	0.87	2.84	0.924	0.245	2.79
-2	0.600	2.386	0.95	2.51	0.922	0.263	2.01
	0.857	2.236	1.14	1.96	0.917	0.336	0.83
	0.970	2.200	✗	✗	✗	✗	0.19
	0	3.000	1.00	3.00	0.964	0.318	π
	1/3	2.941	1.01	2.91	0.963	0.327	2.79
-3	0.600	2.795	1.05	2.66	0.960	0.356	2.01
	0.857	2.535	1.17	2.17	0.954	0.467	0.83
	0.970	2.421	✗	✗	✗	✗	0.19

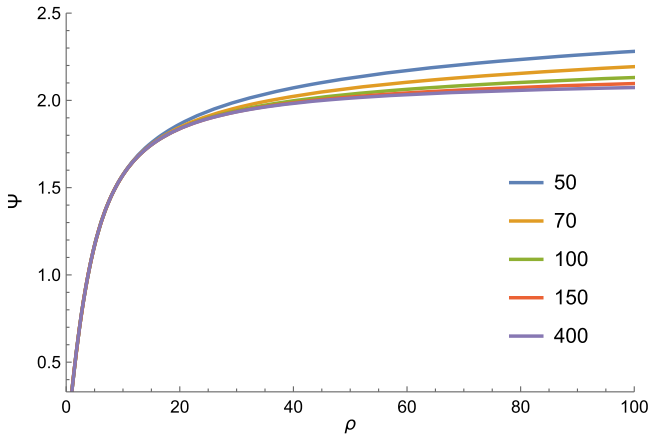

FIG. 6. Plot of the scalar field Ψ [Eqs. (11) and (25)] as a function of the radius in Schwarzschild coordinates (22), (23) with parameters chosen as in Fig. 1. The plots are based on expansions taking into account the first 50, 70, 100, 150 and 400 terms, as indicated by the different colors. The event horizon is located at $\rho = 1$, where $\Psi = b_0 = 1/3$. For the graphs with 100 and more terms, the displayed range of $\rho(= \Omega)$ lies fully within the convergence radius. The fact that Ψ tends asymptotically to a constant means that the physical scalar fields goes for large ρ as $\phi \sim 1/\rho$, in agreement with [16,17]. By considering a series with up to 1000 terms (not displayed here) we have obtained a rough estimate of the asymptotic value of $\Psi \approx 2.13$ (this is, however, an extrapolation based on the value of Ψ at a distance from the horizon of about 10^3 horizon radii, cf. similar comments in Fig. 5). It also follows from the graphs that Ψ (and thus ϕ) does not possess any nodes in the exterior region, again in agreement with the numerical results of [16,17].

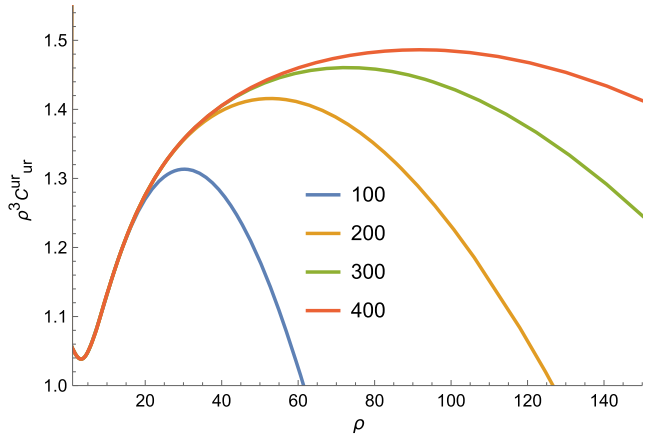

FIG. 7. For any asymptotically AdS metric of the form (22), the Ashtekar-Magnon mass formula [75] boils down to $M = \frac{1}{2}\rho^3 C^{ur}{}_{ur}|_{\rho\to\infty}$ (cf., e.g., [78]), where $C^{ur}{}_{ur}$ is a component of the Weyl tensor (which falls off asymptotically as $C^{ur}{}_{ur} \sim \rho^{-3}$). This is plotted as a function of ρ using expansions with 100, 200, 300 and 400 terms, as indicated by the different colors, and the parameters are chosen as in Fig. 1. The "flat" part of each curve (which in all cases falls within the convergence radius, cf. Figs. 1 and 3) indicates a spacetime region where our series correctly reproduces the asymptotic behavior $\rho^3 C^{ur}{}_{ur} \to$ const. From a series with 1000 terms (not displayed) one can thus extrapolate, in a region around $\rho \approx 200$, an Ashtekar-Magnon mass given approximately by $M \approx 0.77$. Similarly, by choosing the parameters $\Lambda = -3$, $a_0 = 1$, $b_0 = 0.857$ (which correspond to those used in figure 2 of [17]) one would estimate $M \approx 1.17$ (cf. table II), which agrees within 2% with the numerical value obtained in [17] (see also footnote 13).

further noticed that the general upper and lower bounds on ρ_{ps} discussed in [39,60–64] are indeed fulfilled.[10] For comparison, let us observe that the photon sphere of both the BBMB and MTZ black holes is located at $\rho_{ps} = 2M$ (cf. [32,65] for the BBMB case).[11]

In addition, Fig. 5 shows the typical AdS behavior $H \to$ const < 0 for $\rho \to \infty$. Using an expansion with a large number of terms one can obtain an estimate of the asymptotic value of H, and thus compute the angular radius of the black hole shadow (10) for a static observer close to infinity, cf. Table II (it will also be needed in Sec. III B 2 to normalize the timelike Killing vector and thus compute the temperature). Similarly, the behavior of the scalar field Ψ in the exterior region is depicted in Fig. 6, in qualitative agreement with the numerical findings of [16,17]. Also here one can estimate the asymptotic value of Ψ.

A few comments on the notion of mass used above and its values exemplified in Table II are now in order. In an asymptotically AdS spacetime, one can compute the mass M using the Ashtekar-Magnon formula [75] (provided the matter fields have a suitable fall-off [75,76]; cf. [77] for related comments in the presence of a scalar field). However, making computations at conformal infinity with the series method illustrated above means going close or beyond the convergence radius of the solution and becomes therefore extremely challenging. As an example of these difficulties, we plot in Fig. 7 the quantity $\rho^3 C^{ur}{}_{ur}$, which [for an asymptotically AdS metric of the form (22)] should tend to a constant equal to $2M$ for $\rho \to \infty$ [75]. Figure 7 clearly shows that our expansions are unable to reproduce the correct asymptotic behavior for an

[10]It should be emphasized, however, that Refs. [39,60–64] typically assume the weak or even the dominant energy conditions, which can be violated in certain spacetime regions by a black hole sourced by a conformal scalar field (see appendix for more details). Nevertheless, since the same bounds as obtained [39,60–64] appear to be satisfied also here, it would be interesting if those proofs could be extended to cover also the case of a conformal scalar field—however, this goes beyond the scope of the present paper.

[11]In the case $\Lambda = 0$, photon spheres and shadows of black holes with a constant conformal scalar field [46,66–68] have been studied in [69]. For more general asymptotically flat hairy black holes, a bound on the size of the "hairosphere" was obtained in [70] and related to the size of the photon sphere in [71], cf. also [72,73]. Some results for the case $\Lambda \neq 0$ can be found in [73,74].

arbitrarily large ρ.[12] Nevertheless, for each of the curves there exists a range of ρ (within the convergence radius, cf. Figs. 1 and 3) where the curve flattens, thus indicating a spacetime region where the series solution becomes close to reproducing the correct asymptotic behavior. By considering an expansion with a large number of terms, one may thus attempt an extrapolation to compute (a lower bound on) the Ashtekar-Magnon mass—cf. Table II. It follows that, at least for the considered values of the parameters, M grows monotonically with b_0, in agreement with Fig. 5 of [17]. We should stress, however, that further analysis with different (e.g. numerical) methods will be needed to set such kind of estimates on a firmer basis. This goes beyond the scope of this paper.[13]

2. Thermodynamics

Wald's formula enables one to compute the entropy in any diffeomorphism invariant Lagrangian theory [79]. For Lagrangians involving no more than second derivatives of the metric and first derivatives of the matter fields, one has [80–82]

$$\mathcal{S} = -2\pi \oint Y^{abcd}\hat{\epsilon}_{ab}\hat{\epsilon}_{cd}, \qquad Y^{abcd} \equiv \frac{\partial \mathcal{L}}{\partial R_{abcd}}, \tag{38}$$

where the integral is taken with respect to the induced volume element on an arbitrary cross section of the horizon, and $\hat{\epsilon}_{ab}$ is the binormal to the cross section. For the theory (1), (3) (recalling footnote 3) one has $16\pi Y^{abcd} = (1-\phi^2)g^{a[c}g^{d]b}$, while a horizon at $r = r_0$ for metric (7) means $\hat{\boldsymbol{\epsilon}} = \Omega^2 \mathrm{d}u \wedge \mathrm{d}r$. Then one readily finds

$$\mathcal{S} = \frac{\mathcal{A}_h}{4}\left(1 - \frac{b_0^2}{a_0^2}\right), \tag{39}$$

where $\mathcal{A}_h = 4\pi a_0^2$ is the horizon area. The scalar hair thus results in a multiplicative factor which affects the standard area law, making the entropy smaller for a given horizon radius. As mentioned in Sec. III A, $\mathcal{S}$ is positive precisely in the branch $a_0^2 - b_0^2 > 0$. Additionally, let us emphasize that (39) is a closed-form expression (since computed at the horizon, where only the first term of each of the series (25) plays a role), from which one can obtain exact numerical values of the entropy for particular choices of the horizon radius a_0 and the hair parameter b_0. For example, choosing the parameters as in Fig. 1 one obtains $\mathcal{S} = \frac{8\pi}{9}$ (cf. Table II). Modifications to the area law due to nonminimally coupled scalars have been pointed out previously in [83,84] (see also [15,85] for specific examples, and [86,87] for earlier results in $2+1$ dimensions).[14]

Finally, let us compute the temperature associated with a generic Killing vector field $\boldsymbol{\xi} = N\partial_t = -N\partial_u$, for the time being without specifying the normalization constant $N > 0$ ($\boldsymbol{\xi}$ has norm $\xi_b\xi^b = N^2\Omega^2 H$ and is thus timelike future oriented where $H < 0$, and null at the horizon, i.e., for $H = 0$). The surface gravity is defined by $\nabla^a(\xi_b\xi^b) \doteq -2\kappa\xi^a$ [27], where the symbol $\doteq$ denotes equality at the horizon. For the temperature $T = \frac{\kappa}{2\pi}$ one thus finds

$$T = -\frac{Nc_0}{4\pi}. \tag{40}$$

Next, we normalize the Killing field such that $\xi_b\xi^b \sim \frac{\Lambda}{3}\rho^2$ for $\rho \to \infty$ [57] (cf. [88] for further comments). For a specific choice of parameters of the solution, one can employ the asymptotic (approximate) value of H to fix N (Fig. 5) and thus estimate a numerical value of T. For example, with the parameters of Fig. 1 one obtains $T \approx 0.091$ (cf. Table II for different choices of parameters).

IV. CONCLUSIONS

We have studied analytically static, spherically symmetric solutions to AdS-Einstein gravity conformally coupled to a scalar field, in the absence of any self-interaction potential. In the first part of our contribution, we have described how to reduce the field equations to the simple form (16)–(18) by a choice of suitable coordinates (cf. also [22], and [28,29] in a different context). This first result, employed in the rest of the paper, could be useful also in various future studies. Next, we have set up an ansatz (25) for a power series solution of the Eqs. (16)–(18). By analyzing the corresponding indicial equations, we have identified distinct branches of solutions, summarized in Table I. These correspond to expansions at physically different points and may admit different numbers of integration constants, thus describing physically distinct

[12]One arrives at a similar conclusion also by studying the behavior of the dimensionless quantity $\frac{R}{4\Lambda} - 1$, which departs from being zero [the value which should be attained by an exact solution, cf. (5)] as the value of ρ grows "too large" (for example, for a series with 1000 terms, an error no larger than 1% is obtained for $\rho \lesssim 122$).

[13]For values of the parameters similar to those used in figure 2 of [17] (i.e., $\Lambda = -3$ and $b_0 = 0.857$, with our normalization), we extrapolated a value of the Ashtekar-Magnon mass in agreement within 2% with the numerical value obtained in [17] (see also Fig. 5 therein), cf. the captions to our Fig. 7 and table II. For the smaller values $b_0 = 0.6$ and $b_0 = 1/3$ of table II (still with $\Lambda = -3$), we compared M with further numerical data provided to us privately by Eugen Radu (see also Fig. 5 of [17]) and found an agreement within 1%. However, one would obviously need to test whether this agreement still holds on a larger set of values of the parameters.

[14]It may be useful to further observe that formula (39) has been obtained off-shell, and is not modified by adding a self-interaction potential to the theory (1), cf. [66]. Indeed, when specialized to the particular case of the $\Lambda > 0$ MTZ black hole [13] (for which $a_0^2 - b_0^2 < 0$ [46]), it produces a result in agreement with [85], including the negative black hole horizon entropies discussed there (see Ref. [66] for further comments).

solutions. While a detailed study of all possible cases will deserve a separate investigation, in the rest of the paper we have focused on AdS black holes, by considering an expansion around a (necessarily nonextremal) Killing horizon. This gave rise to a solution admitting two integration constants, corresponding to the horizon radius and the value of the scalar field Ψ at the horizon. When the scalar hair vanishes, one recovers the Schwarzschild-AdS vacuum black hole. Properties of the solutions have been described, also using various plots, and compared with the numerical findings of [16,17]. We have, in particular, shown how the coordinates employed throughout this work permit naturally to localize a photon sphere and compute its radius, which is affected by the scalar field but fulfills known general bounds [39,60–64], as well as the associated shadow. In addition, we have briefly discussed the thermodynamics of the solutions. While the entropy can be computed exactly at the horizon, the obtained values of the mass and temperature rely on an extrapolation at large radii, and would need to be further studied by other methods (at least for certain values of the parameters, however, we have found good agreement with the numerics of [17]).

The methods used in this paper can be extended to other contexts, such as black holes with nonspherical horizons, as well as certain extensions of the theory (1). It will be also interesting to study analytically the solitons found numerically in [17]. This will be discussed elsewhere.

ACKNOWLEDGMENTS

I am grateful to Sourya Ray for collaboration at an early stage of this work, for helpful suggestions and for making available to me his work [22] before publication, and to Eugen Radu for useful comments about [17] and for kindly sharing with me large samples of related numerical data. I also thank Vojtěch Pravda for helpful discussions, and Tereza Lehečková for pointing out a typo in Eq. (13) in the first draft of the manuscript. This work has been supported by the Institute of Mathematics, Czech Academy of Sciences (RVO 67985840).

APPENDIX: ENERGY-MOMENTUM TENSOR

The energy-momentum tensor defined by the theory (1) is given by [cf., (5)] $T_{ab} = \phi^2 \tilde{G}_{ab}$, where $\tilde{G}_{ab}$ is the Einstein tensor of the auxiliary metric $\tilde{g}_{ab} = \phi^2 g_{ab}$. The spacetimes considered in this paper are of the form (7) with (11), so that the line element associated with $\tilde{g}_{ab}$ reads

$$\begin{aligned} \mathrm{d}\tilde{s}^2 &= \Psi^2(-2\mathrm{d}u\mathrm{d}r + H\mathrm{d}u^2 + \mathrm{d}\Sigma^2), \\ \mathrm{d}\Sigma^2 &= 2P^{-2}\mathrm{d}\zeta\mathrm{d}\bar{\zeta}, \qquad P = 1 + \frac{1}{2}\zeta\bar{\zeta}. \end{aligned} \tag{A1}$$

After computing $\tilde{G}_{ab}$, the nonzero mixed components of $T^a{}_b$ in the Schwarzschild coordinates (22)–(24) read

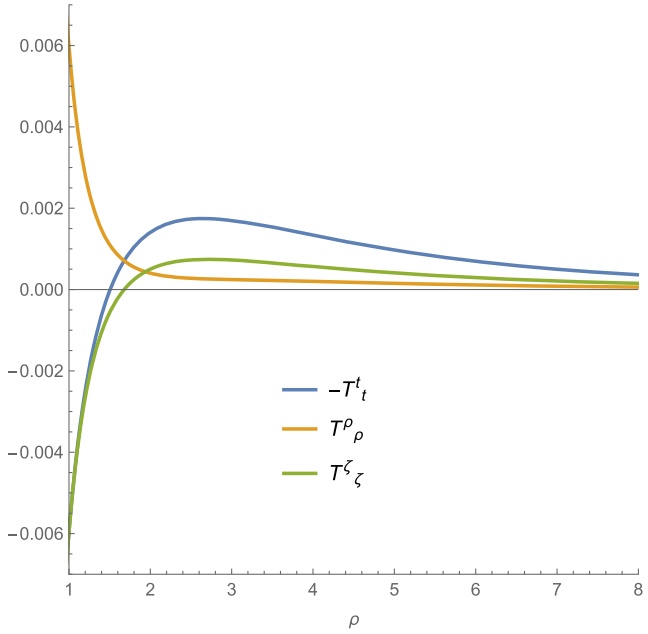

FIG. 8. Plot of the energy-momentum components (A2)–(A4) in the exterior region $\rho > 1$ of the black hole solution (28)–(33) (with parameters as in Fig. 1). The plot is based on an expansion with 400 terms. From the graphs it follows that the energy density is positive for $\rho \gtrsim 1.506$, the WEC holds for $\rho \gtrsim 1.571$, while the DEC for $\rho \gtrsim 1.678$. A similar plot has been obtained numerically in figure 8 of [16].

$$\Omega^4 T^t{}_t = -[\Psi^2 + H'\Psi\Psi' + H(2\Psi''\Psi - \Psi'^2)], \tag{A2}$$

$$\Omega^4 T^\rho{}_\rho = -(\Psi^2 + H'\Psi\Psi' + 3H\Psi'^2), \tag{A3}$$

$$\Omega^4 T^\zeta{}_\zeta = \Omega^4 T^{\bar{\zeta}}{}_{\bar{\zeta}} = \Psi^2 + \Psi(H\Psi')' + H\Psi'^2, \tag{A4}$$

where we have simplified (A4) using (18), such that $T^a{}_a = 0$ (see the comment at the end of Sec. I).

The energy density is given by $-T^t{}_t$ (cf., e.g., [89]). By definition [90], the weak energy condition (WEC) is satisfied in regions where $-T^t{}_t \geq 0$ along with $-T^t{}_t + T^\rho{}_\rho \geq 0$ and $-T^t{}_t + T^\zeta{}_\zeta \geq 0$. The dominant energy condition (DEC) requires that, in addition, also $-T^t{}_t - T^\rho{}_\rho \geq 0$ and $-T^t{}_t - T^\zeta{}_\zeta \geq 0$.

For the black hole solution of Sec. III A one finds at the horizon (i.e., for $H = 0$; as in Sec. III B 2, the symbol $\doteq$ denotes equality at the horizon)

$$T^t{}_t \doteq -\frac{\Lambda}{3}\frac{b_0^2}{a_0^2 - b_0^2} > 0. \tag{A5}$$

Recall that for the hairy solution considered throughout the paper one has $a_0^2 - b_0^2 > 0$, therefore the energy density is negative and thus the WEC is violated at (and, by

continuity, in the vicinity of) the horizon—in agreement with an observation of [16]. One further has $-T^{\zeta}{}_{\zeta} \doteq T^{\rho}{}_{\rho} \doteq T^{t}{}_{t}$ (cf. also [70,89]). However, the plot in Fig. 8 reveals that (at least in a certain region of the parameter space) both the WEC and the DEC are satisfied sufficiently far from the horizon. In particular, the WEC holds precisely outside the photon sphere (at least within the accuracy of the series solution), cf. Fig. 5.

[1] R. Ruffini and J. A. Wheeler, Introducing the black hole, Phys. Today **24**, No. 1, 30 (1971).
[2] M. Heusler, *Black Hole Uniqueness Theorems* (Cambridge University Press, Cambridge, England, 1996).
[3] P. T. Chruściel, J. Lopes Costa, and M. Heusler, Stationary black holes: Uniqueness and beyond, Living Rev. Relativity **15**, 7 (2012).
[4] J. D. Bekenstein, Black hole hair: Twenty-five years after, arXiv:gr-qc/9605059.
[5] M. S. Volkov and D. V. Gal'tsov, Gravitating non-Abelian solitons and black holes with Yang-Mills fields, Phys. Rep. **319**, 1 (1999).
[6] C. A. R. Herdeiro and E. Radu, Asymptotically flat black holes with scalar hair: A review, Int. J. Mod. Phys. D **24**, 1542014 (2015).
[7] M. S. Volkov, Hairy black holes in the XX-th and XXI-st centuries, in *Proceedings of the 14th Marcel Grossmann Meeting on Recent Developments in Theoretical and Experimental General Relativity, Astrophysics, and Relativistic Field Theories* (2017), Vol. 2, pp. 1779–1798, arXiv:1601.08230.
[8] C. G. Callan, Jr., S. R. Coleman, and R. Jackiw, A new improved energy-momentum tensor, Ann. Phys. (N.Y.) **59**, 42 (1970).
[9] B. L. Hu and L. Parker, Anisotropy damping through quantum effects in the early universe, Phys. Rev. D **17**, 933 (1978).
[10] V. Faraoni, *Cosmology in Scalar-Tensor Gravity* (Kluwer Academic Publishers, Dordrecht, 2004).
[11] N. M. Bocharova, K. A. Bronnikov, and V. N. Melnikov, On one exact solution of the set of Einstein and massless scalar field equations, Vestn. Mosk. Univ. Ser. III Fiz. Astron. 706 (1970), in Russian.
[12] J. D. Bekenstein, Exact solutions of Einstein-conformal scalar equations, Ann. Phys. (N.Y.) **82**, 535 (1974).
[13] C. Martínez, R. Troncoso, and J. Zanelli, de Sitter black hole with a conformally coupled scalar field in four dimensions, Phys. Rev. D **67**, 024008 (2003).
[14] C. Martínez, R. Troncoso, and J. Zanelli, Exact black hole solution with a minimally coupled scalar field, Phys. Rev. D **70**, 084035 (2004).
[15] C. Martínez, R. Troncoso, and J. P. Staforelli, Topological black holes dressed with a conformally coupled scalar field and electric charge, Phys. Rev. D **74**, 044028 (2006).
[16] E. Winstanley, On the existence of conformally coupled scalar field hair for black holes in (anti-)de Sitter space, Found. Phys. **33**, 111 (2003).
[17] E. Radu and E. Winstanley, Conformally coupled scalar solitons and black holes with negative cosmological constant, Phys. Rev. D **72**, 024017 (2005).
[18] J. Podolský and M. Ortaggio, Robinson-Trautman spacetimes in higher dimensions, Classical Quantum Gravity **23**, 5785 (2006).
[19] J. Podolský and R. Švarc, Algebraic structure of Robinson-Trautman and Kundt geometries in arbitrary dimension, Classical Quantum Gravity **32**, 015001 (2015).
[20] S. Hervik and M. Ortaggio, Universal black holes, J. High Energy Phys. 02 (2020) 047.
[21] T. Jacobson, When is $g_{tt}g_{rr} = -1$?, Classical Quantum Gravity **24**, 5717 (2007).
[22] S. Ray, Revisiting the static spherically symmetric solutions of gravity with a conformally coupled scalar, arXiv:2406.14345.
[23] J. Oliva and S. Ray, Conformal couplings of a scalar field to higher curvature terms, Classical Quantum Gravity **29**, 205008 (2012).
[24] N. A. Chernikov and E. A. Tagirov, Quantum theory of scalar field in de Sitter space-time, Ann. Inst. Henri Poincaré A **9**, 109 (1968).
[25] S. Deser, Scale invariance and gravitational coupling, Ann. Phys. (N.Y.) **59**, 248 (1970).
[26] L. Parker, Conformal energy-momentum tensor in Riemannian space-time, Phys. Rev. D **7**, 976 (1973).
[27] R. M. Wald, *General Relativity* (The University of Chicago Press, Chicago, 1984).
[28] V. Pravda, A. Pravdová, J. Podolský, and R. Švarc, Exact solutions to quadratic gravity, Phys. Rev. D **95**, 084025 (2017).
[29] J. Podolský, R. Švarc, V. Pravda, and A. Pravdová, Explicit black hole solutions in higher-derivative gravity, Phys. Rev. D **98**, 021502 (2018).
[30] H. Stephani, D. Kramer, M. MacCallum, C. Hoenselaers, and E. Herlt, *Exact Solutions of Einstein's Field Equations*, 2nd ed. (Cambridge University Press, Cambridge, England, 2003).
[31] R. Penrose and W. Rindler, *Spinors and Space-Time* (Cambridge University Press, Cambridge, England, 1986), Vol. 2.
[32] C.-M. Claudel, K. S. Virbhadra, and G. F. R. Ellis, The geometry of photon surfaces, J. Math. Phys. (N.Y.) **42**, 818 (2001).
[33] K. S. Virbhadra and G. F. R. Ellis, Gravitational lensing by naked singularities, Phys. Rev. D **65**, 103004 (2002).
[34] R. d. Atkinson, On light tracks near a very massive star, Astron. J. **70**, 517 (1965).

[35] W. Hasse and V. Perlick, Gravitational lensing in spherically symmetric static space-times with centrifugal force reversal, Gen. Relativ. Gravit. **34**, 415 (2002).
[36] V. Bozza, Gravitational lensing in the strong field limit, Phys. Rev. D **66**, 103001 (2002).
[37] V. Perlick, O. Y. Tsupko, and G. S. Bisnovatyi-Kogan, Influence of a plasma on the shadow of a spherically symmetric black hole, Phys. Rev. D **92**, 104031 (2015).
[38] A. K. Pande and M. C. Durgapal, Trapping of photons in spherical static configurations, Classical Quantum Gravity **3**, 547 (1986).
[39] M. Cvetič, G. W. Gibbons, and C. N. Pope, Photon spheres and sonic horizons in black holes from supergravity and other theories, Phys. Rev. D **94**, 106005 (2016).
[40] V. Perlick, O. Y. Tsupko, and G. S. Bisnovatyi-Kogan, Black hole shadow in an expanding universe with a cosmological constant, Phys. Rev. D **97**, 104062 (2018).
[41] V. Perlick and O. Y. Tsupko, Calculating black hole shadows: Review of analytical studies, Phys. Rep. **947**, 1 (2022).
[42] Y. B. Zel'dovich and I. D. Novikov, Relativistic astrophysics. II., Sov. Phys. Usp. **8**, 522 (1965).
[43] J. L. Synge, The escape of photons from gravitationally intense stars, Mon. Not. R. Astron. Soc. **131**, 463 (1966).
[44] Z. Stuchlík and S. Hledík, Some properties of the Schwarzschild-de Sitter and Schwarzschild-anti-de Sitter space-times, Phys. Rev. D **60**, 044006 (1999).
[45] G. W. Horndeski and D. Lovelock, Scalar-tensor field theories, Tensor (N.S.) **24**, 79 (1972).
[46] G. Dotti, R. J. Gleiser, and C. Martínez, Static black hole solutions with a self-interacting conformally coupled scalar field, Phys. Rev. D **77**, 104035 (2008).
[47] C. Martínez and M. Nozawa, Static spacetimes haunted by a phantom scalar field. I. classification and global structure in the massless case, Phys. Rev. D **103**, 024003 (2021).
[48] H. Piaggio, *An Elementary Treatise on Differential Equations and their Applications* (G. Bell and sons, Ltd., London, 1920).
[49] A. Pravdová, V. Pravda, and M. Ortaggio, Topological black holes in higher derivative gravity, Eur. Phys. J. C **83**, 180 (2023).
[50] J. Podolský, R. Švarc, V. Pravda, and A. Pravdová, Black holes and other exact spherical solutions in quadratic gravity, Phys. Rev. D **101**, 024027 (2020).
[51] B. C. Xanthopoulos and T. Zannias, The uniqueness of the Bekenstein black hole, J. Math. Phys. (N.Y.) **32**, 1875 (1991).
[52] B. C. Xanthopoulos and T. E. Dialynas, Einstein gravity coupled to a massless conformal scalar field in arbitrary space-time dimensions, J. Math. Phys. (N.Y.) **33**, 1463 (1992).
[53] C. Klimčík, Search for the conformal scalar hair at arbitrary *D*, J. Math. Phys. (N.Y.) **34**, 1914 (1993).
[54] T. Zannias, Black holes cannot support conformal scalar hair, J. Math. Phys. (N.Y.) **36**, 6970 (1995).
[55] V. Pravda, A. Pravdová, J. Podolský, and R. Švarc, Black holes and other spherical solutions in quadratic gravity with a cosmological constant, Phys. Rev. D **103**, 064049 (2021).
[56] G. W. Gibbons and S. W. Hawking, Cosmological event horizons, thermodynamics, and particle creation, Phys. Rev. D **15**, 2738 (1977).
[57] S. W. Hawking and D. N. Page, Thermodynamics of black holes in anti-de Sitter space, Commun. Math. Phys. **87**, 577 (1983).
[58] W. Rudin, *Principles of Mathematical Analysis*, 3rd ed. (McGraw-Hill, New York, 1976).
[59] D. Hilbert, Die Grundlagen der Physik, Math. Ann. **92**, 1 (1924).
[60] S. Hod, Upper bound on the radii of black-hole photonspheres, Phys. Lett. B **727**, 345 (2013).
[61] H. Lü and H.-D. Lyu, Schwarzschild black holes have the largest size, Phys. Rev. D **101**, 044059 (2020).
[62] S. Hod, Lower bound on the radii of black-hole photonspheres, Phys. Rev. D **101**, 084033 (2020).
[63] R.-Q. Yang and H. Lü, Universal bounds on the size of a black hole, Eur. Phys. J. C **80**, 949 (2020).
[64] S. Chakraborty, Bound on photon circular orbits in general relativity and beyond, Galaxies **9**, 96 (2021).
[65] Y. Tomikawa, T. Shiromizu, and K. Izumi, On uniqueness of static spacetimes with non-trivial conformal scalar field, Classical Quantum Gravity **34**, 155004 (2017).
[66] M. Nadalini, L. Vanzo, and S. Zerbini, Thermodynamical properties of hairy black holes in *n* spacetimes dimensions, Phys. Rev. D **77**, 024047 (2008).
[67] A. Anabalon and H. Maeda, New charged black holes with conformal scalar hair, Phys. Rev. D **81**, 041501 (2010).
[68] M. Astorino, C metric with a conformally coupled scalar field in a magnetic universe, Phys. Rev. D **88**, 104027 (2013).
[69] M. Khodadi, A. Allahyari, S. Vagnozzi, and D. F. Mota, Black holes with scalar hair in light of the Event Horizon Telescope, J. Cosmol. Astropart. Phys. 09 (2020) 026.
[70] D. Núñez, H. Quevedo, and D. Sudarsky, Black holes have no short hair, Phys. Rev. Lett. **76**, 571 (1996).
[71] S. Hod, Hairy black holes and null circular geodesics, Phys. Rev. D **84**, 124030 (2011).
[72] R. Ghosh, S. Sk, and S. Sarkar, Hairy black holes: Nonexistence of short hairs and a bound on the light ring size, Phys. Rev. D **108**, L041501 (2023).
[73] A. Ishibashi, S. Matsumoto, and Y. Yoneo, A note on no-hair properties of static black holes in four and higher dimensional spacetimes with cosmological constant, Classical Quantum Gravity **41**, 085010 (2024).
[74] R.-G. Cai and J.-Y. Ji, Hairs on the cosmological horizons, Phys. Rev. D **58**, 024002 (1998).
[75] A. Ashtekar and A. Magnon, Asymptotically anti-de Sitter space-times, Classical Quantum Gravity **1**, L39 (1984).
[76] A. Ashtekar and S. Das, Asymptotically anti-de Sitter spacetimes: Conserved quantities, Classical Quantum Gravity **17**, L17 (2000).
[77] A. Anabalon, D. Astefanesei, and C. Martínez, Mass of asymptotically anti-de Sitter hairy spacetimes, Phys. Rev. D **91**, 041501 (2015).
[78] H. Lü, C. N. Pope, and Q. Wen, Thermodynamics of AdS black holes in Einstein-scalar gravity, J. High Energy Phys. 03 (2015) 165.
[79] R. M. Wald, Black hole entropy is the Noether charge, Phys. Rev. D **48**, R3427 (1993).

[80] M. Visser, Dirty black holes: Entropy as a surface term, Phys. Rev. D **48**, 5697 (1993).
[81] T. Jacobson, G. Kang, and R. C. Myers, On black hole entropy, Phys. Rev. D **49**, 6587 (1994).
[82] V. Iyer and R. M. Wald, Some properties of the Noether charge and a proposal for dynamical black hole entropy, Phys. Rev. D **50**, 846 (1994).
[83] J. D. E. Creighton and R. B. Mann, Quasilocal thermodynamics of dilaton gravity coupled to gauge fields, Phys. Rev. D **52**, 4569 (1995).
[84] A. Ashtekar, A. Corichi, and D. Sudarsky, Non-minimally coupled scalar fields and isolated horizons, Classical Quantum Gravity **20**, 3413 (2003).
[85] A.-M. Barlow, D. Doherty, and E. Winstanley, Thermodynamics of de Sitter black holes with a conformally coupled scalar field, Phys. Rev. D **72**, 024008 (2005).
[86] C. Martínez and J. Zanelli, Conformally dressed black hole in $2+1$ dimensions, Phys. Rev. D **54**, 3830 (1996).
[87] M. Henneaux, C. Martínez, R. Troncoso, and J. Zanelli, Black holes and asymptotics of $2+1$ gravity coupled to a scalar field, Phys. Rev. D **65**, 104007 (2002).
[88] J. D. Brown, J. Creighton, and R. B. Mann, Temperature, energy, and heat capacity of asymptotically anti-de Sitter black holes, Phys. Rev. D **50**, 6394 (1994).
[89] A. E. Mayo and J. D. Bekenstein, No hair for spherical black holes: Charged and nonminimally coupled scalar field with self-interaction, Phys. Rev. D **54**, 5059 (1996).
[90] S. W. Hawking and G. F. R. Ellis, *The Large Scale Structure of Space-Time* (Cambridge University Press, Cambridge, England, 1973).